JOURNAL OF VIROLOGY, July 1994, p. 4525–4537
0022-538X/94/$04.00+0

Vol. 68, No. 7

Bgp2, a New Member of the Carcinoembryonic Antigen-Related Gene Family, Encodes an Alternative Receptor for Mouse Hepatitis Viruses

PATRICK NÉDELLEC,[1,2] GABRIELA S. DVEKSLER,[3] EUGENE DANIELS,[4] CLAIRE TURBIDE,[1] BERNARD CHOW,[1] ALEXIS A. BASILE,[3] KATHRYN V. HOLMES,[3] AND NICOLE BEAUCHEMIN[1,2,5,6]*

McGill Cancer Centre[1] and Departments of Medicine,[2] Anatomy,[4] Biochemistry,[5] and Oncology,[6] McGill University, Montreal, Québec, H3G 1Y6, Canada, and Department of Pathology, Uniformed Services University of the Health Sciences, Bethesda, Maryland 20814-4799[3]

Received 6 January 1994/Accepted 25 March 1994

Murine coronaviruses such as mouse hepatitis virus (MHV) infect mouse cells via cellular receptors that are isoforms of biliary glycoprotein (Bgp) of the carcinoembryonic antigen gene family (G. S. Dveksler, C. W. Dieffenbach, C. B. Cardellichio, K. McCuaig, M. N. Pensiero, G.-S. Jiang, N. Beauchemin, and K. V. Holmes, J. Virol. 67:1–8, 1993). The Bgp isoforms are generated through alternative splicing of the mouse *Bgp1* gene that has two allelic forms called MHVR (or mmCGM1), expressed in MHV-susceptible mouse strains, and mmCGM2, expressed in SJL/J mice, which are resistant to MHV. We here report the cloning and characterization of a new Bgp-related gene designated *Bgp2*. The *Bgp2* cDNA allowed the prediction of a 271-amino-acid glycoprotein with two immunoglobulin domains, a transmembrane, and a putative cytoplasmic tail. There is considerable divergence in the amino acid sequences of the N-terminal domains of the proteins coded by the *Bgp1* gene from that of the *Bgp2*-encoded protein. RNase protection assays and RNA PCR showed that *Bgp2* was expressed in BALB/c kidney, colon, and brain tissue, in SJL/J colon and liver tissue, in BALB/c and CD1 spleen tissue, in C3H macrophages, and in mouse rectal carcinoma CMT-93 cells. When *Bgp2*-transfected hamster cells were challenged with MHV-A59, MHV-JHM, or MHV-3, the *Bgp2*-encoded protein served as a functional MHV receptor, although with a lower efficiency than that of the MHVR glycoprotein. The *Bgp2*-mediated virus infection could not be inhibited by monoclonal antibody CC1 that is specific for the N-terminal domain of MHVR. Although CMT-93 cells express both MHVR and Bgp2, infection with the three strains of MHV was blocked by pretreatment with monoclonal antibody CC1, suggesting that MHVR was the only functional receptor in these cells. Thus, a novel murine *Bgp* gene has been identified that can be coexpressed in inbred mice with the *Bgp1* glycoproteins and that can serve as a receptor for MHV strains when expressed in transfected hamster cells.

Murine hepatitis viruses (MHVs) are positive-stranded enveloped RNA viruses of the *Coronaviridae* family (37). MHV infection causes inapparent infection, hepatitis, and respiratory, neurological, and gastrointestinal disorders (4, 42). The first receptor for the MHV-A59 virus (MHVR) was identified on intestinal brush border membranes and liver membranes of MHV-susceptible BALB/c mice (46). MHVR is an isoform of the mouse biliary glycoprotein 1 (*Bgp1*) gene (BgpA or MHVR) of the carcinoembryonic antigen (CEA) gene family. It is also expressed in C57BL/6 and C3H mice (10). Transfection of MHVR cDNA into MHV-resistant hamster cells made the cells susceptible to infection with MHV-A59, MHV-JHM, and MHV-3 (11). A monoclonal antibody (MAb CC1) directed against the N-terminal domain of MHVR blocked virus attachment to murine fibroblasts, thus preventing infection, and partially protected neonatal BALB/c mice against MHV-A59 (36, 45).

In the case of humans, a single *BGP* gene has been mapped in a large cluster of at least 22 CEA-related genes on chromosome 19 (40). The human *BGP* gene can generate at least 12 different transcripts by alternative splicing (2, 3, 18). A rat *Bgp* gene (ecto-ATPase) displays many of the features of the human *BGP* gene (24). Although no regulatory elements have yet been mapped, expression of the rat *Bgp* gene can be modulated by hormonal regulation (39). Our group has cloned and characterized a *Bgp* gene (*Bgp1*) in mice that displays the same attributes as the rat and human *BGP* genes, including generation of many splice variants (10, 22, 24a, 41, 48). Four isoforms of *Bgp1* have been reported (22); they will be referred to as the $Bgp1^a$ gene products. A variant of *Bgp1* (originally designated mmCGM2 or BgpB) was initially thought to be an alternate splice variant of the same gene but was later shown to be a codominant allele of the *Bgp1* gene (10, 41). Isoforms of this variant, expressed in SJL/J and outbred CD1 mice (10, 22, 41, 48), will be referred to as $Bgp1^b$ gene products. The BGP proteins are expressed in a wide variety of tissues and cell types. Epithelial cells in intestine, kidney, liver, uterus, and stomach tissue and endothelial and hematopoietic cells express one or more BGP isoforms (6, 25). It is at present unclear which BGP isoforms or splice variants are involved in the numerous cellular functions associated with these proteins. Four isoforms of $Bgp1^a$ or $Bgp1^b$ have been shown to serve as receptors for MHV after either transfection of their cDNA into MHV-negative BHK cells or into SJL/J embryonic fibroblasts (10). The highest levels of expression of *Bgp1* proteins are found in intestine and liver tissues, which are some of the principal target tissues for MHV replication (45).

In this paper, we report on the characterization of a second mouse *Bgp* gene (*Bgp2*), which is expressed in BALB/c brain, colon, and spleen tissue, C3H macrophages, and SJL/J colon and liver tissue. From the rectal carcinoma cell line CMT-93,

* Corresponding author. Phone: (514) 398-3541. Fax: (514) 398-6769.

TABLE 1. Nomenclature of mouse CEA-related genes, transcripts, and proteins

Gene	Transcript and/or protein (reference)[a]			Structure[b]	GenBank accession number(s)
	Montreal	Bethesda	Los Angeles		
Bgp1[a]	BgpA (22), mmCGM1a (23)	MHVR1 (11)	mmCGM1 (49), MHVR1 (47)	N1[a], A1[a], B1[a], A2[a], TM, S	X15351, M77196
	BgpC (22)	MHVR1 (2d)[c] (10)	mmCGM2 B6[d] (48)	N1[a], A2[a], TM, S	X67278, M96934
	BgpD (22)	MHVR1 $(4d)_L$[e] (10)		N1[a], A1[a], B1[a], A2[a], TM, L	X67279
	BgpG (22)	MHVR1$(2d)_L$		N1[a], A2[a], TM, L	X67282
Bgp1[b]	BgpB (22), mmCGM2 (41)	mmCGM2(2d) (10)	mmCGM2 (49) MHVR2 (47)	N1[b], A2[b], TM, S	X53084
	BgpE (22)	mmCGM2(4d) (10)	mmCGM1 SJL[f] (48)	N1[b], A1[b], B1[b], A2[b], TM, S	X67280, M96935
	BgpF (22)	mmCGM2$(4d)_L$		N1[b], A1[b], B1[b], A2[b], TM, L	X67281
	BgpH (22)	mmCGM2$(2d)_L$		N1[b], A2[b], TM, L	X67283
Bgp2	Bgp2C (this paper)	Bgp2(2d)		N2, A2, TM, S	X76085

[a] Names of cities refer to locations of research groups having published mouse CEA-related sequences.
[b] N, N-terminal domain; N1[a] and N1[b], N-terminal domains of the *Bgp1* a and b alleles, respectively; N2, N-terminal domain of the *Bgp2* gene; A1, B1, and A2, C2-set Ig domains; TM, transmembrane domain; S, short (10 amino acids) intracytoplasmic tail; L, long (73 amino acids) intracytoplasmic tail.
[c] 2d, two Ig domains.
[d] B6, C57BL/6 mouse.
[e] 4d, four Ig domains.
[f] SJL, SJL/J mouse.

we have cloned a *Bgp2* cDNA that encodes a protein with two immunoglobulin (Ig)-like domains. Although the gene organization is conserved, the N-terminal and A2 domain sequences are divergent from those of the previously reported *Bgp* isoforms, suggesting that this novel *Bgp* gene may have arisen by recombination and gene duplication of a prototype *Bgp* gene. We also demonstrate that the *Bgp2*-encoded protein can serve as a receptor for three strains of MHV.

MATERIALS AND METHODS

Nomenclature. Table 1 summarizes the names previously used to designate products of the mouse *Bgp1* gene and shows the names that will be used in this paper for the purpose of clarity. The genomic locus of mmCGM1 or MHVR will be called *Bgp1*[a]. The protein with four Ig domains and a short cytoplasmic domain encoded by *Bgp1*[a] is called MHVR(4d) or BgpA, and the splice variant that joins the first and fourth Ig domains is called MHVR(2d) (10) or BgpC (22). The genomic locus of the allele of the *Bgp1*[a] gene expressed in SJL/J and CD1 mice will be called *Bgp1*[b]; its protein product was formerly named mmCGM2 (41) or BgpB. The new *Bgp* gene reported here expresses a third type of N-terminal domain. Because this is, in fact, the second *Bgp* gene described, we have named it *Bgp2*; its protein isoform bearing two Ig domains, described herein, will be referred to as Bgp2C.

Genomic Southern analysis. Genomic DNA isolated from BALB/c, C57BL/6, and SJL/J spleen tissue was purchased from Jackson Laboratories, Bar Harbor, Maine. An 8-μg portion of genomic DNA was digested with *Eco*RI, *Bam*HI, and *Hin*dIII, separated on a 1% agarose gel, and transferred to GeneScreen Plus membranes (Du Pont, NEN Research Products, Montreal, Canada). The filters were hybridized with a 391-bp *Nco*I restriction fragment from the *Bgp1* gene proximal promoter region (24a) and with a 153-bp PCR-generated fragment corresponding to residues 270 to 363 of the *Bgp2* cDNA (see Fig. 5B).

Labeling of probes and hybridization. DNA restriction fragments were separated on low-melting-point agarose and labeled with [α-^{32}P]dATP by random priming (13). Oligonucleotides were synthesized on a Pharmacia synthesizer at the Sheldon Biotechnology Centre, McGill University, and end labeled with [γ-^{32}P]ATP as described previously (32). Filters were hybridized as previously described (23) by using either 10^6 cpm of labeled restriction fragments per ml or 2×10^6 cpm of oligonucleotides per ml. Washes were done either in 0.1× SSC solution–0.1% sodium dodecyl sulfate (SDS) (1× SSC is 0.15 M NaCl plus 0.015 M sodium citrate) at 65°C for 30 min when restriction fragments were used or in 6× SSC–0.1% SDS for 30 min at temperatures corresponding to 5°C below the calculated melting temperature of the oligonucleotides.

Genomic cloning and characterization. To obtain a full-length gene sequence for the mouse *Bgp2* gene, the following two BALB/c mouse genomic libraries were screened: a λEMBL3 mouse genomic library, obtained from Clontech, Palo Alto, Calif., and a pWE15 cosmid library, graciously provided by Edwin Geissler, Boston, Mass. A total of 10^6 independent phage clones and 3.6×10^5 independent cosmid clones were plated on Nytran filters (Schleicher & Schuell, Keene, N.H.) which were hybridized in duplicate with an *Eco*RI-*Sac*I restriction fragment corresponding to the leader, the N-terminal domain, and the A1 and B1 internal domains of the BgpA cDNA (23). The *Bgp2* gene was identified in the various clones obtained from the first round of screening by hybridizing *Hin*dIII-restricted DNA prepared from these clones with an *Nco*I restriction fragment from the *Bgp1* gene proximal promoter region (24a) and a γ-^{32}P-labeled 21-mer oligonucleotide specific to the BgpB cDNA that encodes the N domain (formerly mmCGM2) (oligonucleotide 5 in Table 2) (41). The restriction map of the phage 7.3 clone was defined by using a LambdaMap kit available from Promega. The first 5 exons of the *Bgp2* gene were localized in phage 7.3 and cosmid 10.2 to a 2.4-kb *Bam*HI restriction fragment which was isolated, subcloned into a pBluescript SK+ vector (Stratagene), and sequenced.

DNA sequencing. Restriction fragments were subcloned into unique sites of the pBluescript SK+ phagemid (Stratagene). Two micrograms of plasmid DNA was denatured, and 30 ng of either T7 or T3 promoter primers or internal primers was annealed to the DNA to sequence both strands by the dideoxy chain termination method (33) using T7 DNA polymerase (Pharmacia). DNA sequencing was also performed directly on DNA prepared from cosmid clones by using essentially the same method, but 150 ng of specific oligonucleotides was annealed to the DNA. Sequences were analyzed by using the DNAsis, Prosis (Pharmacia), and Devereux (9) programs.

TABLE 2. Sequences of oligonucleotides used in this study

Oligonucleotide no.	Sequence	Orientation[a]	Position in cDNA (nt)[b]
1	5′ GGAGAATCAATTCTGCTATGAA 3′	S	6–27
2	5′ GGCTTAGCAGTAGTGTTGG 3′	S	44–62
3	5′ ATGGCTTTTCCACTCCACGC 3′	S	213–232
4	5′ CGAGACTCCCTTCATCAT 3′	A	270–288
5	5′ GTCTTATTAGTGCCTGTTAC 3′	A	345–365
6	5′ GGTGTTGGTGACTTGGAG 3′	A	543–561
7	5′ AACAATGATACTCTTCTAATC 3′	S	636–656
8	5′ GATTAGAAGAGTATCATTGTT 3′	A	636–656
9	5′ CAGAATAGACCCTATTAAGAGGGAAGATGCCGG 3′	S	695–726
10	5′ CCGGCATCTTCCCTCTTAATAGGGTCTATTCTG 3′	A	695–726
11	5′ GACTCAACATATGACATTTCA 3′	S	801–821
12	5′ TGAAATGTCATATGTTGAGTC 3′	A	801–821
13	5′ AGCGAGACTTCCTGGAACAGAGGCG 3′	A	891–915
14	5′ CCCAGCAACCCAACC 3′	S	986–1000
15	5′ GGCTCCAGGATCCACCTTTTCTTC 3′	A	1239–1263
16	5′ TTGATACCTCACTCTCAGCCA 3′	A	
17	5′ ACACTACGGCTATAGACAAAGA 3′	S	Bgp1[a]
18	5′ GTAGACTCCCATATCCTTCATGG 3′	A	435–458
19	5′ AGACTACAACAGGGCCTG 3′	S	Bgp1[b]

[a] S, sense; A, antisense.
[b] Nucleotide numbers are those in Fig. 5B.

Polymerase chain reaction amplifications. Exon-intron localization was performed by PCR amplification with exon-specific oligonucleotides listed in Table 2. Reactions were incubated in a 100-μl total volume containing 50 ng of cosmid 10.2 template DNA in 20 mM Tris · Cl (pH 8.8), 10 mM KCl, 2 mM $MgSO_4$, 10 mM ammonium sulfate, 0.1% Triton X-100, 0.1 μg of bovine serum albumin, 0.2 mM deoxynucleoside triphosphates, 20 pmol of phosphorylated primers, and 2 U of Vent DNA polymerase (New England Biolabs, Beverly, Mass.). Primers were annealed at 50°C for 2 min, and chain extension was performed at 72°C for 3 min for a total of 30 cycles. The resulting PCR fragments were separated on a 0.8% agarose gel, extracted, and cloned into the pCR-Script SK+ vector (Stratagene) as recommended by the supplier.

RNA preparation. Total cellular or tissue RNA was extracted with guanidine isothiocyanate and then centrifuged through a cesium chloride gradient, as previously described (23). Poly(A)$^+$ RNA was prepared by two passages through oligo(dT) cellulose columns (Collaborative Research, Bedford, Mass.) (5). RNA was also prepared from BALB/c and SJL/J tissues and from thioglycolate-elicited C3H and SJL/J peritoneal macrophages with RNA Stat-60 (Tel-Test "B" Inc., Friendswood, Tex.) according to the manufacturer's instructions.

RNase protection assays and Northern (RNA) analysis. RNase protection assays were performed by using three different fragments of the *Bgp2* gene, an *Acc*I fragment present in the exon encompassing the N-terminal domain (nucleotides [nt] 319 to 455 in Fig. 5B), a *Taq*I fragment of the A2 exon (nt 600 to 750 in Fig. 5B), and a 153-bp fragment of the second exon corresponding to the region of greatest divergence from the *Bgp1* gene (nt 270 to 363 in Fig. 5B). These fragments were inserted into the pBluescript SK+ vector and sequenced to determine the appropriate orientation. After linearization, the inserts were transcribed for 1 h at 37°C by using either T7 or T3 RNA polymerase and [^{32}P]UTP under conditions described in reference 17. The transcription products were submitted to digestion with 10 U of RNase-free DNase (Boehringer Mannheim, Dorval, Canada) for 15 min at 37°C, and the resulting transcripts were ethanol precipitated. A 10^5-cpm portion of labeled probe was added to either 20 μg of total RNA or 5 to 20 μg of poly(A)$^+$ RNA from different tissues or cell lines and hybridized at 50°C for 18 h. The hybrids were treated with 40 μg of RNase A per ml and 100 U of RNase T1 for 30 min at 37°C, and then they were treated with 100 ng of proteinase K and 0.25% SDS for 30 min at 37°C and ethanol precipitated. The resulting hybrids were electrophoretically separated by being passed through 8 M urea–6% polyacrylamide gels, which were dried and exposed to XAR film. Northern analysis was performed on 2.2 M formaldehyde–1.5% agarose gels essentially as described by McCuaig et al. (23).

Reverse transcription-polymerase chain amplification reaction. Cloning of the *Bgp2* cDNA was performed by reverse transcription reactions, as described by McCuaig et al. (22), by using avian myeloblastosis virus reverse transcriptase (Life Sciences, St. Petersburg, Fla.), 15 μg of poly(A)$^+$ RNA extracted from mouse rectal carcinoma cell line CMT-93, and oligonucleotide 16 (Table 2). PCR amplification was performed by using either Vent DNA polymerase (New England Biolabs) or *Taq* DNA polymerase (Pharmacia) on single-stranded cDNA with a primer (oligonucleotide 1 in Table 2) designed for the putative 5′ untranslated exon of the *Bgp2* gene and another primer (oligonucleotide 15 in Table 2) located in the 3′ untranslated region, as described above. The resulting fragments were separated on a 1% agarose gel, and the DNA was extracted and cloned into the pCRII vector (Invitrogen, San Diego, Calif.). Additionally, 2 μg of total RNA extracted from the CMT-93 cells, BALB/c brain tissue, or peritoneal macrophages was reverse transcribed by using primer 6 (Table 2) and random primers and then amplified by PCR with primer 2 (Table 2), which hybridizes to the 5′ untranslated region, and primer 6 (Table 2). Primers used in the PCRs were designed to amplify both *Bgp1* and *Bgp2* cDNAs with the same efficiency. After amplification, the products were separated in duplicate on a 1% agarose gel and transferred to Nytran membranes. Each membrane was probed with a ^{32}P-labeled oligonucleotide specific for the *Bgp1*[a] cDNA (oligonucleotide 17 in Table 2) or the *Bgp2* cDNA (oligonucleotide 3 in Table 2), and possible cross-hybridization with the *Bgp1*[a] or *Bgp2* cDNA was monitored. For amplification of SJL/J and BALB/c colon tissue

cDNAs, an antisense primer found within the second exon of the *Bgp* gene (oligonucleotide 18 in Table 2) and a primer specific to the 5′ untranslated region exon (oligonucleotide 2 in Table 2) were used, and the PCR products were electrophoresed in triplicate, Southern blotted, and hybridized to either *Bgp1*^{a}- (oligonucleotide 17), *Bgp1*^{b}- (oligonucleotide 19), or *Bgp2*-specific (oligonucleotide 3) oligonucleotides as indicated in the legend to Fig. 4.

Viruses and cells. All MHV strains were propagated in the 17 Cl 1 line of spontaneously transformed BALB/c 3T3 cells and plaque assayed in L2 cells (38). Vaccinia virus strain vTF7-3 was kindly provided by B. Moss (National Institutes of Health, Bethesda, Md.) and propagated in CV-1 cells. The CMT-93 cells, obtained from the American Type Culture Collection, and the BHK-21 line of baby hamster kidney fibroblasts were grown in Dulbecco's modified Eagle's minimal essential medium supplemented with heat-inactivated 10% fetal calf serum and antibiotics (GIBCO Laboratories, Grand Island, N.Y.). Mouse colon carcinoma cell lines CT 36 and CT 51 (8) were a generous gift from Michael Brattain, and mouse breast carcinoma Mm5MT cells were obtained from the American Type Culture Collection.

Assays of transient expression in hamster cells and virus challenge. For transient expression assays, the *Bgp2* cDNA was excised from the TA vector and subcloned into the *Hin*dIII-*Not*I sites of pRcCMV (Invitrogen). A *Bgp2-Bgp1*^{a} hybrid cDNA molecule was constructed by replacing the first 71 amino acids encoded by the *Bgp1*^{a} cDNA with those encoded by the *Bgp2* cDNA, taking advantage of the common *Bam*HI site and the *Hin*dIII site present in the polylinker of the vector. Transfections into hamster (BHK) cells were performed by using lipofectAMINE (Life Technologies, Gaithersburg, Md.) as indicated by the manufacturer. Thirty to thirty-five hours posttransfection, the cells were challenged for 1 h at 37°C with MHV-A59, MHV-3, or MHV-JHM at a multiplicity of infection of 1 PFU per cell. For MAb CC1 protection experiments, BHK cells transiently transfected with the *Bgp2* cDNA or CMT-93 cells grown on coverslips were treated with a 1:2 dilution of anti-receptor MAb CC1 hybridoma supernatant or control MAb to an irrelevant antigen for 1 h prior to and during virus adsorption (except for MHV-JHM, for which the antibody was not present during the virus adsorption). At 12 h postinoculation, the cells on coverslips were fixed with cold acetone. Viral antigens in the cytoplasm were detected by immunofluorescence with a 1:50 dilution of mouse polyclonal anti-MHV-A59 convalescent serum followed by rhodamine-labeled goat anti-mouse IgG as described by Dveksler et al. (11).

Immunoblot and virus overlay protein blot analysis. BHK cells were infected with vaccinia virus expressing T7 RNA polymerase (vTF7-3) at a multiplicity of infection of 10 PFU per cell. At 3 h after vTF7-3 inoculation, plasmids containing the cDNA of interest or plasmids with no insert were transfected into the cells by using lipofectAMINE. At 24 h after transfection, the cells were lysed with 0.3 ml of radioimmunoprecipitation assay buffer (0.1 M NaCl, 0.001 M EDTA [pH 7.4], 0.1% Nonidet P-40, 0.1% deoxycholate, 1% aprotinin). The proteins were electrophoresed on SDS–8% polyacrylamide gels, transferred to nitrocellulose membranes, and, after being blocked, were incubated with either a 1:500 dilution of rabbit polyclonal anti-MHVR 655 antibody preadsorbed with vaccinia virus-infected BHK cells (11), a 1:50 dilution of MAb CC1 followed by a rabbit anti-mouse antibody (7), a 1:100 dilution of rabbit antibody to human CEA (DAKO, Carpinteria, Calif.), or a 1:1,000 dilution of rabbit polyclonal anti-mouse *Bgp1* antibody 231 (23). The blots were then incubated with 10^5 cpm of ^{125}I-labeled staphylococcal protein A, washed, and exposed to film. For virus overlay protein blot assays the blots were incubated with MHV-A59 followed by goat antibody against the virus spike protein S and radiolabeled staphylococcal protein A as described by Boyle et al. (7).

RESULTS

Identification of *Bgp2*, a novel CEA-related gene. In the characterization of the regulatory region of the gene encoding the mouse CEA-related gene family member called Bgp (*Bgp1* or MHVR1; Table 1), a unique *Nco*I proximal promoter probe of 391 bp was generated. This probe was previously used to define regulatory controls involved in the down-regulation of *Bgp* gene expression in transformed cells and had identified three distinct fragments of 1.35, 3.8, and 6.5 kb in *Hin*dIII-digested genomic DNA (30). When the probe was hybridized to either *Bam*HI-, *Eco*RI-, or *Hin*dIII-digested genomic DNA of three inbred mouse strains (BALB/c, SJL/J, and C57BL/6), a complex pattern of bands was observed (Fig. 1A). The BALB/c and C57BL/6 patterns were indistinguishable in all digests. In the *Bam*HI digests from the three mouse strains, two fragments of 2.2 and 2.4 kb were apparent, with the longest one being present in two copies as determined by the relative radioactive intensities. However, the *Eco*RI digests produced three hybridizing fragments of 2.3, 8.6, and 10.0 kb with the BALB/c and C57BL/6 strains, while fragments of 2.3, 8.6, and >15.0 kb were apparent in SJL/J DNA digests. Among the *Hin*dIII digests, three fragments (1.35, 3.8, and 6.5 kb) were detected in the BALB/c and C57BL/6 digests, while SJL/J *Hin*dIII digests produced hybridizing fragments of 3.5, 3.8, and 6.4 kb. We have found that a 1.35-kb *Hin*dIII fragment is contained within the proximal promoter, first exon, and first intron of the BALB/c mouse *Bgp1* gene (24a). Therefore, this restriction pattern suggests the existence of three highly homologous Bgp-related genes in the BALB/c and C57BL/6 mice. The SJL/J mouse however, has a restriction fragment length polymorphism such that the 1.35-kb *Hin*dIII fragment is absent and a new 3.5-kb fragment is present (Fig. 1A, lane 2). Dveksler et al. have previously shown that the *Bgp1*^{a} gene products are not expressed in this mouse strain (10).

The *Bgp2* gene assignment was confirmed after the exon encompassing the N-terminal domain of this new gene was cloned. A 153-bp fragment of the *Bgp2* DNA located at nt 270 to 363 (Fig. 5B), in a region that shows maximum divergence from other published *Bgp* DNA sequences (22), was hybridized with genomic DNA from the three mouse strains. This fragment bound to a 2.4-kb *Bam*HI fragment, an 8.6-kb *Eco*RI band, and a 3.8-kb *Hin*dIII band of the BALB/c, C57BL/6, and SJL/J DNA (Fig. 1B). Thus, the *Bgp2* gene does not appear to be grossly rearranged in the SJL/J mouse, as the same hybridization pattern was observed in the three mouse strains.

Cloning and characterization of the *Bgp2* gene. DNA prepared from several cosmid and phage clones isolated in the first screening of the genomic libraries for the mouse *Bgp1* gene (24a) was digested with *Hin*dIII and probed with the *Nco*I proximal promoter fragment to detect the presence of a 3.8-kb fragment specific to the *Bgp2* gene. Phage 7.3 and cosmid 10.2 demonstrated the appropriate fragment. After several restriction enzyme sites within the phage 7.3 insert were mapped, a 2.4-kb *Bam*HI band which hybridized strongly to both a *Bgp1*^{b}-specific oligonucleotide (oligonucleotide 5 in Table 2) and an *Eco*RI-*Bam*HI fragment of the *Bgp1*^{a} (BgpA) cDNA encompassing the 5′ untranslated region, the leader sequence, and the N-terminal domain was identified. This fragment was subcloned and sequenced. Several nucleotide differences were

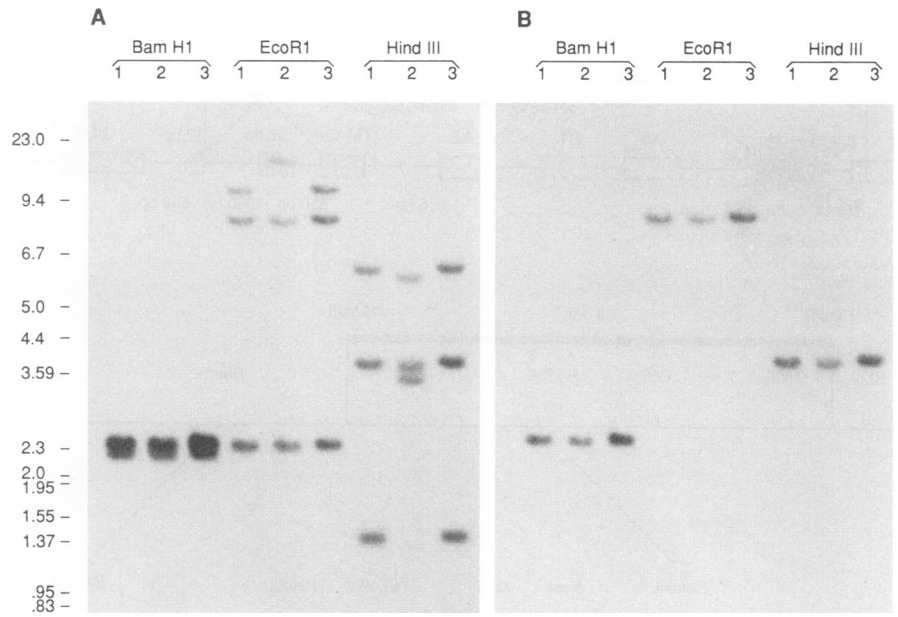

FIG. 1. Genomic analysis of BALB/c, SJL/J, and C57BL/6 mouse *Bgp* genes. An 8-μg portion of genomic DNA obtained from either BALB/c (lanes 1), SJL/J (lanes 2), or C57BL/6 (lanes 3) mice was digested with either *Bam*HI, *Eco*RI, or *Hin*dIII. Resulting fragments were then electrophoresed in a 0.8% agarose gel, transferred to a GeneScreen Plus membrane, and probed with either a ^{32}P-labeled BALB/c *Bgp1* 391-bp *Nco*I proximal promoter probe (A) or a ^{32}P-labeled 153-bp PCR-generated fragment corresponding to residues 270 to 363 of the *Bgp2* cDNA (B). The blots were washed in a 0.1× SSC solution containing 0.1% SDS at 65°C for 30 min. Markers on the left are in kilobases.

found when the fragment was compared with the MHVR cDNA (11); some of these nucleotide changes led to amino acid substitutions. The *Bgp2* gene was not a pseudogene, since an intron was present between the first two exons, no in-frame stop codons were found within the putative coding region, and this gene was expressed (see below). Identification of this new exon in an inbred strain that has a $Bgp1^b$ allele (the SJL/J mouse) showed that this gene was a novel *Bgp* gene family member.

We then characterized the downstream organization of *Bgp2*. Exons 1 and 2 were first localized on the mouse *Bgp2* gene by sequencing of the 2.4-kb *Bam*HI fragment isolated from phage 7.3. Their DNA sequences exhibited 76% homology to that of the *Bgp1* gene. Most of the first intron was also sequenced and demonstrated greater than 90% DNA sequence homology to the first intron of the mouse $Bgp1^a$ (24a) and human *BGP* (15) genes. Similar results were obtained when the upstream regulatory sequences were compared (data not shown), suggesting overall conservation of the 5′ region during evolution. Other putative exons were localized by directly sequencing DNA of the cosmid 10.2 insert with oligonucleotides designed for the *Bgp1* gene and cDNAs (oligonucleotides 5, 9, 10, and 14 to 16 in Table 2). Comparisons of exon sequences with the DNA sequences of the *Bgp2* cDNA clones obtained after reverse transcription PCR (RT-PCR) (see below) showed them to be identical. The mouse *Bgp2* gene (Fig. 2) has an overall organization very similar to that of the mouse *Bgp1* gene (24a), the rat *Bgp* gene (called ecto-ATPase; 24), and the human *BGP* gene (2, 15). An uncharacterized gap of 4.3 kb separates the L/N and A2 exons of the *Bgp2* gene. By using a probe encompassing the A1 and B1 domains of $Bgp1^a$ cDNA, putative A1 and B1 exons have been detected upon Southern analyses of the 4.3-kb region. However, cloning of a four-domain *Bgp2*-encoding cDNA that would include these two exons after RT-PCR amplification of RNA extracted from several mouse tissues with primers in the N and A2 exons of the *Bgp2* gene has so far been unsuccessful.

Another feature of the *Bgp* gene organization that is well conserved throughout evolution is found in the exon structure at the 3′ end of the gene. In the human (2) and rat (24) *Bgp* genes as well as in the mouse *Bgp1* gene (24a), the long intracytoplasmic tail of either 71 or 73 amino acids is generated by alternative splicing and insertion of a 53-bp exon which disrupts the original reading frame. Although the amino acid sequences vary slightly for each species, the overall homology of this long intracytoplasmic domain is the most conserved feature of the *Bgp* genes. The mouse *Bgp2* gene also exhibits the same features, although a *Bgp2* transcript encoding a long intracytoplasmic tail has not yet been identified.

The lengths of the introns shown in Fig. 2 and Table 3 were determined by PCR amplification using primer pairs found within each exon. The DNA sequences of exon-intron splice junctions are shown in Table 3. These conform to splice donor and acceptor consensus sequences. As previously demonstrated with the human *CEA* and *BGP* genes (2, 15, 16, 34, 43), the identity of the last amino acid encoded by an exon depends on the completion of the codon with one or two nucleotides from the next exon (Table 3).

Tissue-specific expression of the *Bgp2* gene. Because of the high level of homology of the *Bgp2* DNA sequences to those of the *Bgp1* alleles and those of the mouse *Cea* gene complex known as homologs of the pregnancy-specific genes (31), RNase protection assays were used to define the expression patterns of the *Bgp2* mRNA(s) in mouse tissues and cell lines. Three different fragments were used for this analysis (Fig. 3A). (i) A *Taq*I fragment, subcloned from the A2 domain, coincides with the region exhibiting greatest divergence from similar domains within the mouse *Bgp* and *Cea* genes; (ii) an *Acc*I fragment was produced after digestion of DNA encoding the *Bgp2* N-terminal domain and corresponds to the latter two-

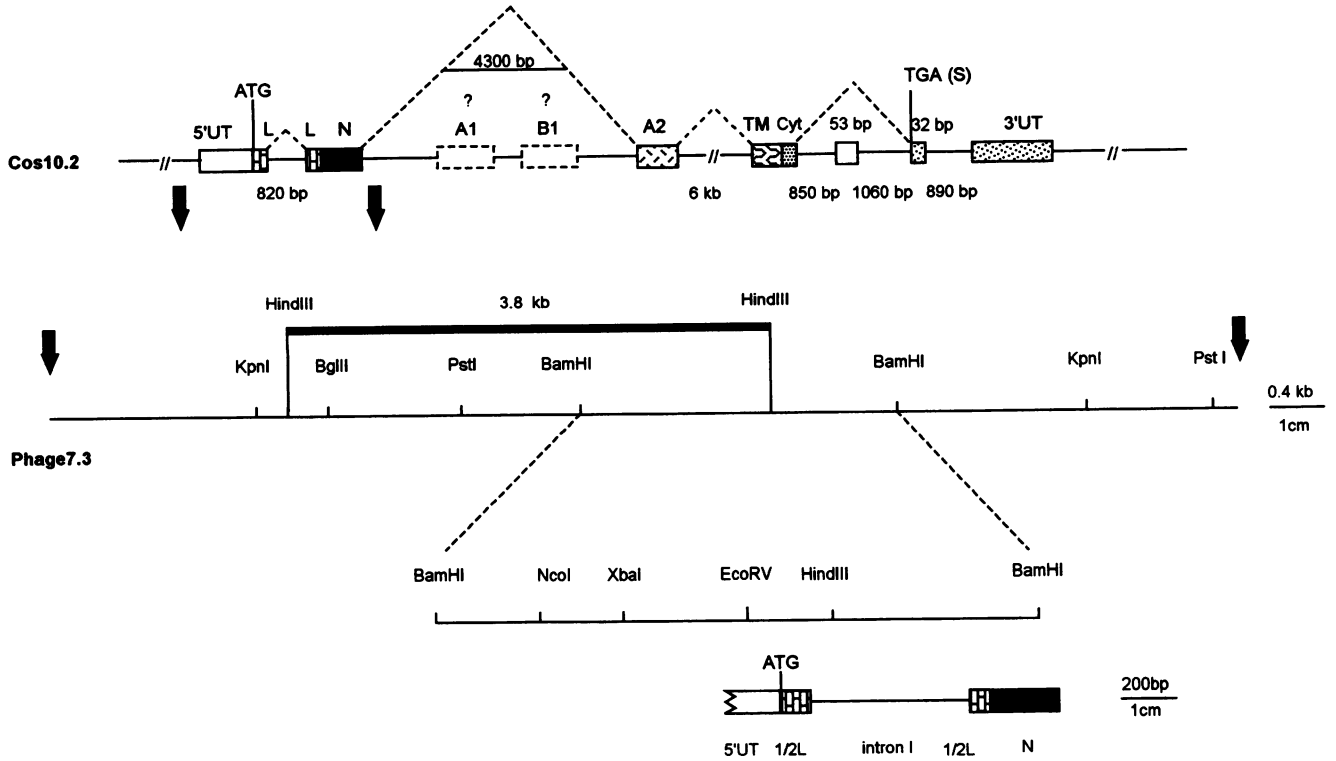

FIG. 2. Genomic organization of the *Bgp2* gene. The *Bgp2* gene was cloned from mouse cosmid and phage libraries as described in Materials and Methods. The full-length *Bgp2* gene was found on cosmid clone 10.2, and its genomic organization was established by cloning and sequencing restriction fragments hybridizing to the *Bgp1* cDNA or PCR fragments amplified with exon-specific primers. On the basis of homology with *BGP* genes of humans and other *Bgp* genes of mice and as indicated by its use of consensus splice acceptors and donors, the *Bgp2* gene appears to have seven exons. These correspond to the 5′ untranslated region (5′UT) and half leader (L) sequence, half leader and N-terminal domain (N), a C2-set Ig domain (A2), a linker and transmembrane exon encoding eight putative intracytoplasmic amino acids (TM), a 53-bp open reading frame which tentatively could encode 19 amino acids of a long intracytoplasmic tail (Cyt), and a 32-bp exon as well as another longer exon encoding a region of the 3′ untranslated region (3′UT). Putative A1 and B1 exons have been identified by hybridization to similar exons of the *Bgp1* gene but have not been precisely localized and are shown as dashed boxes. The initiation of translation codon (ATG) as well as the stop codon (TGA) are indicated. The dashed lines indicate the possible alternate splicing of exons to generate the *Bgp2* transcript. The sizes of the introns were deduced from the PCR fragments, which were sequenced and shown to be exon specific. The region of the cosmid 10.2 (Cos10.2) clone encompassing the phage 7.3 clone is delineated by thick arrows. The partial gene organization on the phage 7.3 clone is shown at the bottom of the figure. Restriction sites were mapped by using a LambdaMap kit or defined through DNA sequencing. The dark line indicates the position of the 3.8-kb *Hin*dIII genomic fragment hybridizing to the *Bgp1 Nco*I proximal promoter probe. The 2.4-kb *Bam*HI fragment encoding the first and second exons as well as restriction sites referred to in the text is enlarged at the bottom of the panel.

TABLE 3. Exon-intron organization of the *Bgp2* gene

Exon	Exon size (bp)	Exon and intron sequence[a] 5′ splice donor 3′ splice acceptor	Approximate intron size (bp)	Amino acid interrupted
1	ND[b]	CTACTGCTCACAG..gtaagg L L L T	tcttag.CCAGGCTTTTA A S L L	820	A
2	369	TTTCATGTACACA..gtaagt F H V H	ccacag.AGCCAGTGACT K P V T	ND	K
5	275	CTGGAAGTAATAT..gtgagg L E V I	tgacag.TTGACTCAACA F D S T	6,000	F
6	116	AGGAAGTCTCGCTG.gtagga R K S R *	atttag..[GGGAAGTGAC	850	Stop codon
7	53	GCCTCCAACCACA]..gtaagt	ccctag..ATCTGGCTCCT	1,060	
8	32	TCTCCTAACAAGgtgagc	tttcagGTGGATGACGTC	890	

[a] Capital letters represent exon nucleotide sequences; lowercase letters are intron nucleotide sequences. Single-letter code amino acid sequences are indicated under the exon nucleotide sequences. Dots represent nucleotides necessary to complete the codon. Italicized letters in brackets represent a 53-bp open reading frame which could encode part of a putative long intracytoplasmic tail. Lines joining the short intracytoplasmic tail to the 32-bp exon represent the actual splicing occurring in the *Bgp2* mRNA.

[b] ND, not determined.

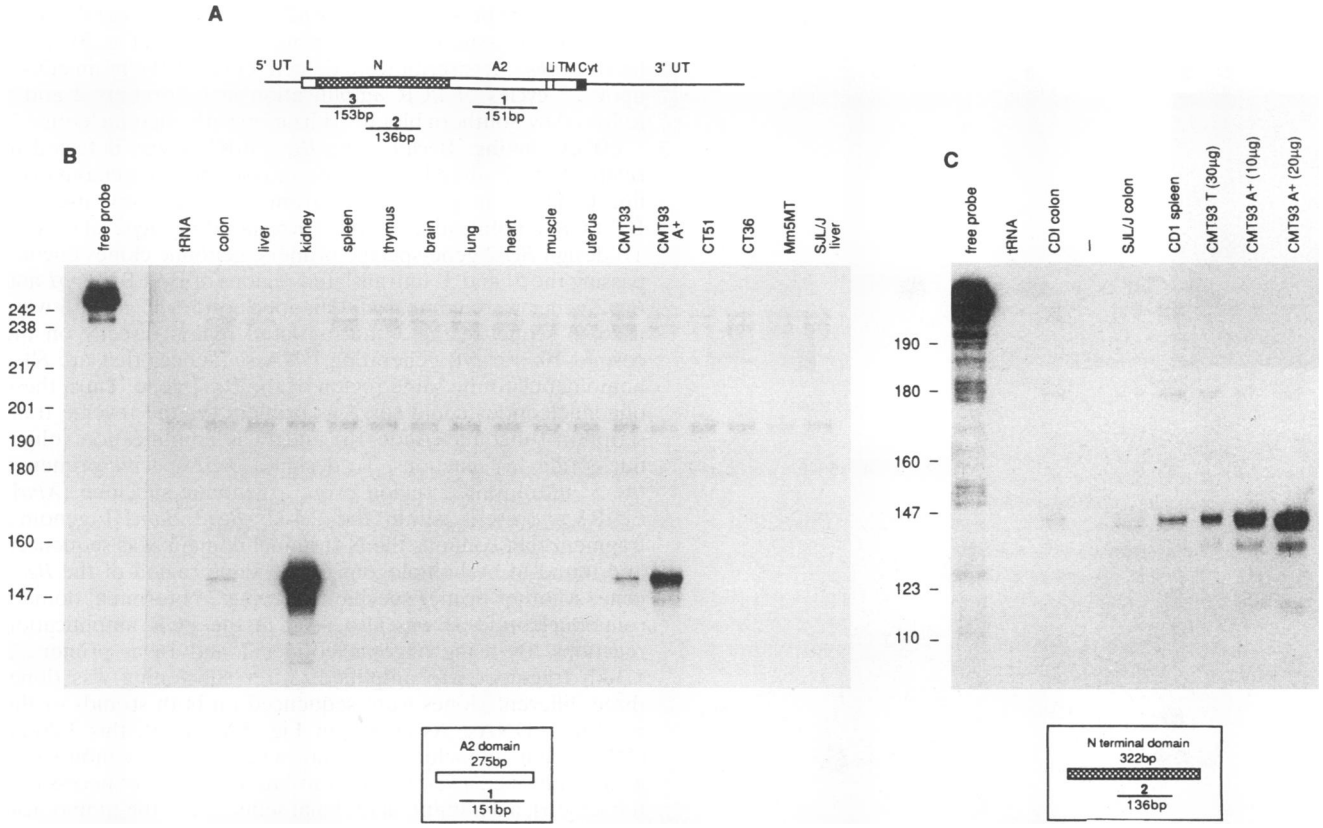

FIG. 3. RNase protection assays performed to define *Bgp2* mRNA expression patterns. The RNA probes used in the RNase protection assays are shown in panel A. These correspond to a 151-bp *Taq*I fragment of the A2 exon, a 136-bp *Acc*I fragment encompassing a region of the N-terminal domain, and a 153-bp PCR-generated fragment corresponding to nt 270 to 363 of the *Bgp2* cDNA, the region of highest divergence from the same region of the *Bgp1* gene. A total of 10^5 cpm of ^{32}P-labeled probes was hybridized at 50°C for 18 h to 20 μg of total RNA or 10 to 20 μg of poly(A)$^+$ RNA from the designated tissues or cell lines. The RNA duplexes were submitted to RNase digestion as described in Materials and Methods and electrophoresed on an 8 M urea–6% acrylamide gel. The markers at the left of panels B and C are in base pairs. The first ten tissues from the left in panel B were taken from BALB/c mice.

thirds of the N domain; and (iii) a 153-bp fragment was generated by PCR amplification using the 2.4-kb *Bam*HI genomic fragment (consisting of the 5′ untranslated region-, leader-, and N-terminal domain-encoding exons) as the template. This PCR fragment represents the region of greatest divergence of the *Bgp2* cDNA from sequences available for other members of the mouse *Cea* gene family. Figure 3B shows that the RNA probe specific for the A2 domain (probe 1 in Fig. 3A) protected a 151-nt fragment (Fig. 3B) as expected on the basis of the nucleotide sequence of the cDNA (Fig. 5B) in BALB/c colon and kidney RNA and in the (C57BL/6 × Af)F_1 progeny-derived CMT-93 rectal carcinoma RNA. Upon longer exposure of the blot, faint signals were detected in BALB/c spleen and SJL/J liver RNA. No other tissue or cell line expressed RNA that reacted with this probe, even after a prolonged exposure of the blot to a Fuji Phosphorimager plate. A second probe, corresponding to the latter two-thirds of the N-terminal domain (probe 2 in Fig. 3A), also protected a 136-bp RNA fragment in CD1 spleen and colon tissue, SJL/J colon tissue, and CMT-93 cells (Fig. 3C). Similar results were obtained with the 153-bp probe corresponding to the divergent region of the N-terminal domain (probe 3 in Fig. 3A; data not shown). No signals were detected upon Northern analysis using either 20 μg of total tissue RNA or 10 μg of poly(A)$^+$ RNA from the other cell lines tested with either the 153-bp N-terminal domain restriction fragment or *Bgp2* gene-specific oligonucleotides. Since RNase protection assays have revealed signals in RNAs from some mouse tissues and cell lines, while the Northern analysis was negative, *Bgp2* mRNA(s) is probably present in low abundance in these tissues and cell lines.

To confirm that the SJL/J mouse did, in fact, express these transcripts, an RT-PCR amplification was performed on SJL/J colon RNA, using BALB/c colon RNA as a control. Oligonucleotides common to the first and second exons encoded in the *Bgp1*^{a} and the *Bgp1*^{b} transcripts and the *Bgp2* gene were used to amplify 450-bp fragments from these samples (Fig. 4A, lanes 2 and 3). As shown in Fig. 4, when the PCR fragments were hybridized with either a *Bgp1*^{a}-specific oligonucleotide (oligonucleotide 17 in Table 2) (Fig. 4B) or a *Bgp1*^{b}-specific oligonucleotide (oligonucleotide 19 in Table 2) (Fig. 4C), only the BALB/c colon and SJL/J colon cDNAs, respectively, displayed positive signals. However, when the same blot was hybridized with a *Bgp2*-specific oligonucleotide (oligonucleotide 3 in Table 2) (Fig. 4D), both BALB/c and SJL/J RNAs exhibited positive signals, indicating that *Bgp2* mRNA(s) is expressed in both mouse strains.

To determine whether macrophages express the *Bgp2* mRNA, RNA was prepared from thioglycolate-elicited C3H peritoneal macrophages and amplified by RT-PCR with primers 2 and 6. Since these primers amplify both the *Bgp1* and

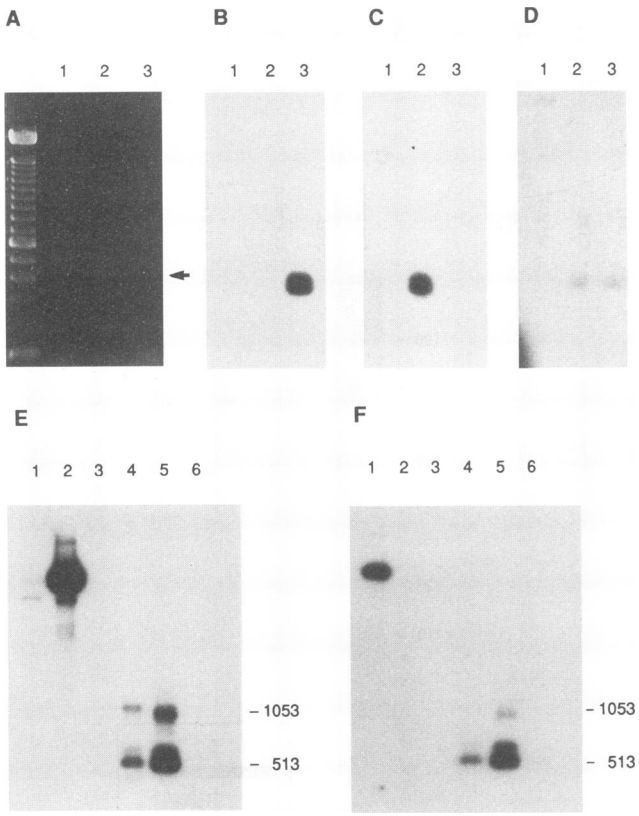

FIG. 4. Expression of the *Bgp2* mRNA in BALB/c, SJL/J, and C3H mouse tissues. RNAs extracted from BALB/c and SJL/J colon tissue were submitted to RT-PCR amplification using oligonucleotides 18 (N-terminal domain) and 2 (5′ untranslated region) in Table 2. PCR products were electrophoresed in triplicate on a 1% agarose gel, transferred to Nytran membranes, and probed with oligonucleotides specific for the *Bgp1*^{a} cDNAs (oligonucleotide 17, panel B), the *Bgp1*^{b} cDNAs (oligonucleotide 19, panel C), or the *Bgp2* cDNA (oligonucleotide 3, panel D). Lanes 1 of panels A through D represent an H_2O control for the PCR; lanes 2 contain SJL/J colon cDNA; and lanes 3 contain BALB/c colon cDNA. The ladder in panel A is the 100-bp marker (Life Technologies). Alternatively, 2 μg of total RNA extracted from CMT-93 cells or C3H thioglycolate-elicited macrophages was submitted to RT-PCR amplification using primers 2 and 6 in Table 2. These primers were designed to amplify both the *Bgp1* and *Bgp2* cDNAs. The CMT-93-derived PCR products were amplified for either 20 (E and F, lanes 3) or 25 (E and F, lanes 4) cycles. The PCR products were treated as described above, and the membranes were hybridized with a *Bgp1*^{a}-specific oligonucleotide (oligonucleotide 17, panel E) or a *Bgp2*-specific oligonucleotide (oligonucleotide 3, panel F). Lanes 1 of panels E and F represent a *Bgp2* cDNA control, while lanes 2 contain a *Bgp1*^{a} cDNA control. Lanes 5 contain PCR products from C3H macrophages, and lanes 6 are H_2O controls for the PCRs. The 513- and 1,053-bp products correspond to PCR products of cDNAs exhibiting two and four Ig domains, respectively.

Bgp2 cDNAs with the same efficiency, the expression of the mRNAs was analyzed with oligonucleotide probes 17 and 3, respectively. Figure 4 shows that C3H macrophages (panels E and F, lanes 5) expressed the two-domain and four-domain isoforms of *Bgp1*^{a} mRNAs and at least a two-domain *Bgp2* mRNA isoform. A hybridization signal that could account for a four-domain *Bgp2* isoform was also detected. Further analyses and cloning of the putative *Bgp2* four-domain isoform are required to determine its expression.

Although expression of the *Bgp2* transcript was not detected in the brain tissue by RNase protection assay (Fig. 3B), low levels of *Bgp2* transcript were detected in BALB/c brain cDNA upon 35 cycles of PCR amplification using primers 2 and 6 followed by Southern blot hybridization with oligonucleotide 3.

cDNA cloning. Because the *Bgp2* mRNA was detected in relatively high abundance in the mouse rectal carcinoma cell line CMT-93, poly(A)$^+$ RNA from these cells was used for RT-PCR amplification of the corresponding *Bgp2* cDNA(s). To design *Bgp2* gene-specific primers, genomic clones encompassing the 5′ and 3′ untranslated regions of BALB/c *Bgp1* and *Bgp2* genes were compared. Oligonucleotides 15 and 16 were used to sequence the 3′ untranslated region directly on the cosmid 10.2 insert, generating DNA sequences that are 88% homologous to the same region of the *Bgp1* gene. Thus, these oligonucleotides could serve as primers for the reverse transcription (oligonucleotide 16) and PCR amplification (oligonucleotide 15) reactions. To design a *Bgp2*-specific primer in the 5′ untranslated region exon, a genomic subclone (*Xba*I-*Eco*RV), present within the 2.4-kb *Bgp2* *Bam*HI genomic fragment that contains the N-terminal domain, was sequenced and found to be homologous to the same region of the *Bgp1* gene. Another primer specific to the *Bgp2* N-terminal domain (oligonucleotide 3) was also used in the PCR amplification reactions. By using oligonucleotides 1 and 16 as primers, a 1.3-kb fragment was amplified. After subcloning was done, three different clones were sequenced on both strands of the resulting cDNAs. As shown in Fig. 5A and B, this 1.26-kb cDNA fragment included the known features of the mouse *Cea* gene family, i.e., a 98-bp 5′ untranslated region (not necessarily full length), a 34-amino-acid signal sequence, a 108-amino-acid N-terminal domain, a 92-amino-acid A2 domain, a 31-amino-acid linker region and transmembrane domain followed by an 8-amino-acid putative intracytoplasmic tail, and a 3′ untranslated region containing a $(CA)_{26}$ dinucleotide repeat. The nucleotide sequence of this cDNA corresponded perfectly to the exon nucleotide sequences of the *Bgp2* gene.

The Bgp amino acid sequence comparisons shown in Fig. 5C highlight some of the distinctive features of this new protein. Two nucleotide substitutions within the signal sequence lead to two amino acid changes at the same positions in the Bgp1^a and Bgp1^b proteins. The N-terminal domain presents interesting characteristics and is the most divergent region. The first 37 amino acids of the *Bgp2*-encoded protein differ markedly from the corresponding amino acids of the *Bgp1*-encoded proteins (Fig. 5C). Twenty amino acid substitutions, seven of which affect charge or size, are obvious. The latter two-thirds of this N-terminal domain is 88% similar to that of the *Bgp1*^{b} allele while exhibiting only 72% similarity to that of the *Bgp1*^{a} allele. The Bgp2 N-terminal domain displays two N-linked glycosylation sites (thin underline in Fig. 5C) at positions identical to those of sites found within Bgp1^b. The A2 domain of Bgp2 also conserves two N-linked glycosylation sites, although the central site of Bgp1 is positioned closer to the 5′ end of Bgp2 through mutations. The middle of the A2 domain of Bgp2 varies markedly from the conserved sequences found in the BALB/c and SJL/J alleles with 17 discrepancies out of 32 amino acids. The two cysteines thought to be involved in intramolecular disulfide bonds, as well as key amino acids involved in conformational stabilization of the immunoglobulin fold (44), are conserved. The linker and transmembrane domains are shorter by four amino acids (indicated by dashes in the sequence) than the Bgp1^a and Bgp1^b proteins and exhibit mainly conserved substitutions. An eight-amino-acid putative intracytoplasmic tail was also observed. To maximize alignments, three gaps have been inserted in the Bgp1^a and Bgp1^b sequences before

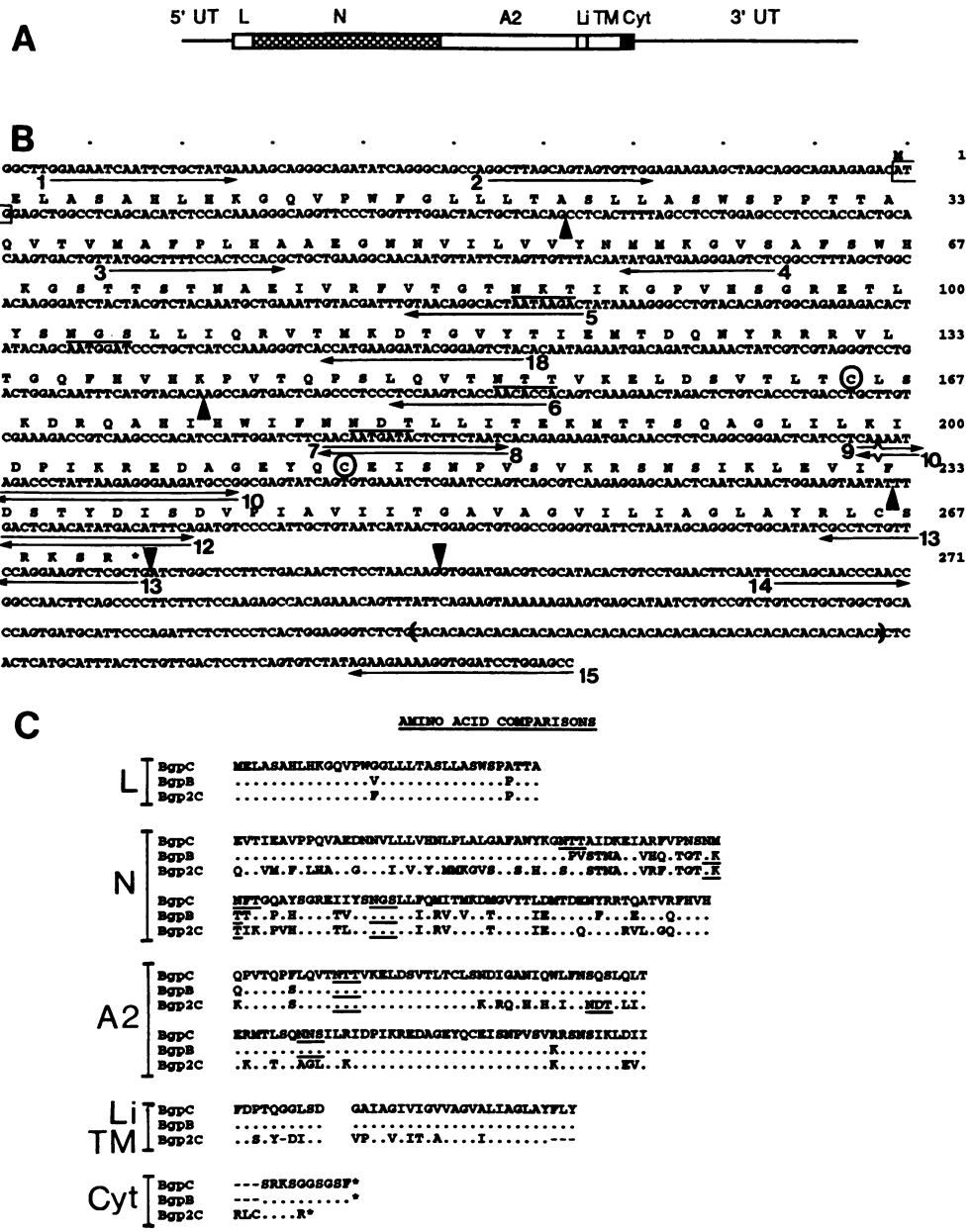

FIG. 5. Nucleic acid and predicted amino acid sequences encoded by the *Bgp2* gene. (A) The structure of the *Bgp2* cDNA is shown. The PCR-amplified cDNA comprises a 98-bp 5′ untranslated region (5′UT), a 34-amino-acid leader sequence (L), a 108-amino-acid N-terminal domain (N), a 92-amino-acid C2-set Ig domain (A2), a 9-amino-acid linker region (Li), a 22-amino-acid transmembrane domain (TM), and an 8-amino-acid intracytoplasmic tail (Cyt) followed by a 345-bp partial 3′ untranslated region (3′UT). (B) The nucleic acid sequence of the *Bgp2* cDNA (numbered on the left) and its deduced amino acid sequence (single-letter code; numbered on the right) are shown. The ATG translation initiation codon is boxed, and the TGA stop codon is identified by *. The four potential N-linked glycosylation sites are underlined. The cysteine residues potentially involved in disulfide bond formation are circled. The $(CA)_{26}$ tract is enclosed in parentheses. Arrows and numbers under the nucleic acid sequence indicate the positions of some of the oligonucleotides referred to in the text and in Table 2. Large arrowheads correspond to exon borders. (C) Comparison of the BgpC, BgpB, and Bgp2C predicted proteins. Potential N-linked glycosylation sites are underlined. Dashes in the sequences indicate gaps introduced into the sequences to maximize alignments. Protein domains referred to in panel A are indicated on the left of the sequences.

the SRKS sequence (Fig. 5C). The sequence of the short intracytoplasmic domain of Bgp2 is different from those of the $Bgp1^a$ and $Bgp1^b$ proteins; this difference results from a substitution (G-915 → T-915) within the last codon of this *Bgp2* exon, which generates a stop codon and an intracytoplasmic domain shorter than those of the $Bgp1^a$ and $Bgp1^b$ proteins by five amino acids.

The *Bgp2*-encoded protein functions as a receptor for MHV. In an attempt to determine the molecular weight of the protein encoded by the *Bgp2* mRNA, lysates of *Bgp2*-transfected BHK

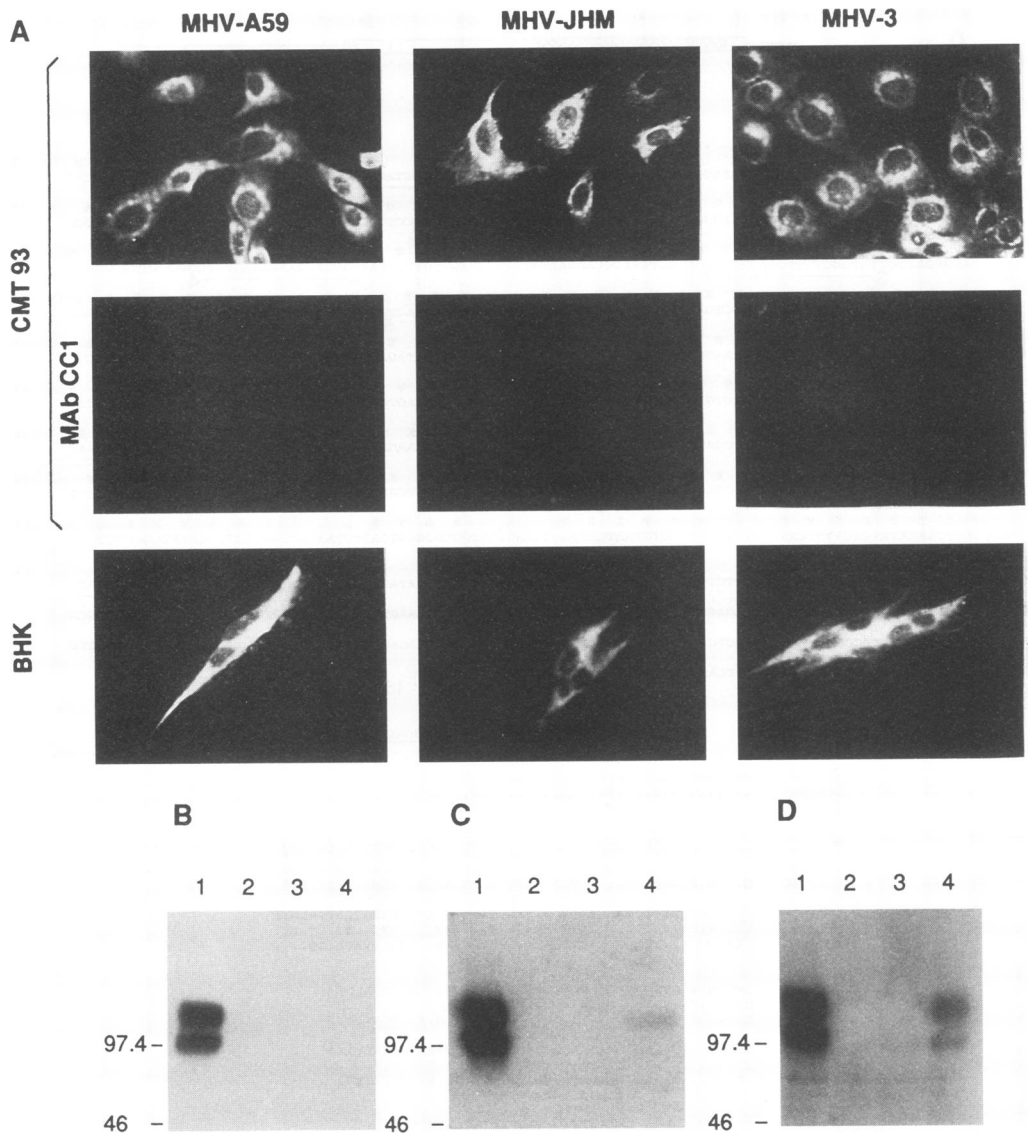

FIG. 6. (A) Immunofluorescence of MHV antigens in CMT-93 cells or *Bgp2*-transfected BHK cells. CMT-93 cells were grown on coverslips and either not treated (top row) or treated for 1 h and during virus adsorption (second row) with a 1:2 dilution of MAb CC1 hybridoma supernatant. *Bgp2*-transiently transfected BHK cells (third row) and CMT-93 cells were then challenged for 1 h at 37°C with MHV-A59, MHV-JHM, and MHV-3 at a multiplicity of infection of 1. Viral antigens were detected 12 h after virus inoculation by using a mouse polyclonal anti-MHV-A59 serum and rhodamine-labeled goat anti-mouse IgG. (B through D) Immunoblot analysis of BHK transfected cells. BHK cells were transfected with either a plasmid containing the $Bgp1^a$ (MHVR) cDNA (lanes 1), a plasmid with no insert (lanes 2), a plasmid containing the *Bgp2* cDNA (lanes 3), or a plasmid containing the *Bgp2-*$Bgp1^a$ hybrid cDNA (lanes 4) by using LipofectAMINE. After 24 h, the cells were lysed and the proteins were electrophoresed on SDS-PAGE gels and transferred to nitrocellulose membranes. The blots were incubated with MAb CC1 followed by rabbit anti-mouse antibody (panel B), anti-MHVR antibody (655) (panel C), or an anti-Bgp antibody (231) (panel D). The blots were then incubated with ^{125}I-protein A, washed, and exposed to film. Positions of molecular size standards (in kilodaltons) are shown to the left of each immunoblot.

cells were immunoblotted with MAb CC1 (36) (Fig. 6B); two anti-MHVR polyclonal antibodies, 655 (11) (Fig. 6C) and 231 (23) (Fig. 6D); and a commercially available polyclonal anti-human CEA antibody that cross-reacts with MHVR (data not shown). None of these antibodies bound to the *Bgp2*-encoded protein in immunoblots (Fig. 6B through D, lanes 3). A chimeric protein that consists of 71 amino acids of the Bgp2 protein followed by the remaining 353 amino acids of the four-domain MHVR coding sequence was not recognized by MAb CC1 (Fig. 6B, lane 4) but was recognized by the three polyclonal antibodies tested (Fig. 6C and D, lanes 4). Thus, the available antisera to murine Bgps did not detect the Bgp2 protein in immunoblots. Intestinal brush border membranes isolated from BALB/c but not SJL/J mice bind MHV-A59 in a virus overlay protein blot assay (7). Since transcripts encoding the Bgp2 protein were detected in colon tissue of both the BALB/c and SJL/J strains, we investigated whether the *Bgp2*-encoded protein could bind MHV-A59 in this assay. The Bgp2 protein was not recognized by MHV-A59 in a virus overlay protein blot assay (data not shown).

To determine whether the *Bgp2* cDNA encodes a functional MHV receptor glycoprotein, this clone was transiently trans-

fected into MHV-resistant BHK cells under the transcriptional control of the CMV promoter. Transfected cells were challenged with MHV-A59, MHV-3, and MHV-JHM. As shown in Fig. 6A, viral antigens developed in the cytoplasm of some of the transfected cells, indicating that the *Bgp2*-encoded protein served as a receptor for each of the three MHV strains tested. Although infected cells were detected in each of four independent experiments, the number of infected BHK cells transfected with the *Bgp2* cDNA was consistently much lower than those of BHK cells transfected in the same experiment with equivalent amounts of the cDNAs encoding the two-domain or four-domain MHVR glycoproteins cloned into the same expression vector. We then investigated whether pretreatment of the *Bgp2*-transfected cells with the anti-MHVR MAb CC1 prevented infection mediated by the *Bgp2*-encoded protein. Neither MAb CC1 nor an unrelated MAb of the same isotype was able to protect the *Bgp2*-transfected cells from virus infection, whereas, as previously reported, MAb CC1 protected cells expressing MHVR isoforms from infection with the three MHV strains (10, 11) (Fig. 6A). Thus, the N-terminal domain of Bgp2 is sufficiently different from $Bgp1^a$ isoforms that MAb CC1 does not bind to it. Because CMT-93 cells expressed transcripts of both MHVR and Bgp2, we used MAb CC1 to determine which Bgp is used as a receptor in CMT-93 cells. MAb CC1 completely protected CMT-93 cells from infection with MHV-A59, MHV-3, and MHV-JHM (Fig. 6A). Thus, the $Bgp1^a$ protein isoforms were the only functional receptors in CMT-93 cells.

DISCUSSION

Structure and expression of the mouse *Bgp2* gene. Two highly polymorphic alleles, $Bgp1^a$ and $Bgp1^b$, of the *Bgp1* gene on mouse chromosome 7 encode numerous glycoprotein isoforms that can serve as receptors for MHV strains (10, 11, 28, 45, 48, 49). Some of these glycoproteins play a role in cell adhesion (23, 29, 41). We have identified a new murine gene related to *Bgp1* that is coexpressed with *Bgp1* in tissues of inbred mice. The restriction pattern obtained upon digestion of DNA isolated from SJL/J, BALB/c, and C57BL/6 mice followed by hybridization to a proximal promoter probe of *Bgp1* suggested the existence of at least three *Bgp* genes. We report here the identification of one of the two new genes, named *Bgp2*. Genomic and cDNA clones of *Bgp2* were obtained from BALB/c mice and from the CMT-93 murine cell line, respectively. Analysis of various fragments of the DNA and the upstream regulatory region and introns of the DNA and the 5′ and 3′ untranslated regions of the cDNA showed that the structure of the *Bgp2* gene closely resembles that of *Bgp1* (2, 15, 24a). These observations suggest that the *Bgp1* and *Bgp2* genes arose from duplication of a common ancestral gene. The relative order of *Bgp1* and *Bgp2* on mouse chromosome 7 is being defined by using a YAC insert of chromosome 7.

The structural features of the *Bgp2* cDNA and its predicted protein product are like those of the mouse *Bgp1* gene as well as those of rat and human *BGP* cDNAs and proteins that include two immunoglobulin-like domains. Common features include a long signal sequence, an N-terminal domain that is salt bridged and resembles a variable Ig domain, a C2-set Ig domain bearing two cysteine residues that are believed to form intrachain disulfide bonds, a transmembrane domain, and a putative intracytoplasmic tail.

The most striking difference between the *Bgp2* cDNA and the $Bgp1^a$ and $Bgp1^b$ cDNAs lies in the first 37 amino acids of the N-terminal domain, which contains 22 amino acid changes, including many nonconservative substitutions. The remainder of the N-terminal domain is more similar to that of $Bgp1^b$ than that of $Bgp1^a$. In Bgp2, the N-terminal domain contains two potential N-linked glycosylation sites in the same positions as sites found in $Bgp1^a$ and $Bgp1^b$. $Bgp1^a$ has one additional N-linked glycosylation site in the N-terminal domain. The second Ig domain of Bgp2 also shows significant differences from the two *Bgp1* allele products. In particular, one potential N-linked glycosylation site is moved from the center toward the distal part of the domain, which could affect the conformation of the protein. The putative transmembrane and intracytoplasmic domains of Bgp2 are shorter than those of the *Bgp1* allele proteins. These marked differences in the amino acid sequence of the Bgp2 protein compared with those of the Bgp1 proteins, particularly the changes in the N-terminal domain, may have important effects on the functions of the protein. Dveksler et al. showed that the N-terminal domain of Bgp1 contains the sites that bind MHV S glycoprotein and the protective anti-receptor MAb CC1 (12), and the N-terminal domain is important for the cell adhesion functions of other CEA-related glycoproteins (27, 50). The extensive amino acid changes between Bgp1 and Bgp2 proteins in this important functional region suggest that evolutionary divergence of the genes may have progressed to the point that the proteins that they encode now recognize different cellular ligands and may serve different cellular functions. Such divergent proteins might also differ in the ability to serve as receptors for MHV.

The natural cellular ligands for Bgp1 and Bgp2 proteins have not yet been identified, although some Bgp1 glycoproteins exhibit homophilic cell adhesion. Other cellular functions attributed to two rat Bgps that differ markedly in their N-terminal domains (20, 26) include an enzymatic ecto-ATPase activity (20, 44), transport of bile acids (35), definition of hepatocyte polarity by differentiation antigens during embryogenesis (14), and activity as receptors in a signal transduction cascade associated with the insulin receptor or protein kinase A or C (1, 3, 20, 21).

The expression of *Bgp2*-encoded transcripts in different mouse tissues varies considerably and is markedly different from the expression of *Bgp1* transcripts as shown by RNase protection assays and RT-PCR amplification. $Bgp1^a$ transcripts are abundantly expressed in the colon and liver tissue of BALB/c and outbred CD1 mice, while the *Bgp2* transcript is only expressed at low levels in the colon tissue of BALB/c and CD1 mice. Low levels of expression of the *Bgp2* transcript were found in BALB/c brain and spleen tissue, but no expression of the *Bgp2* mRNA was detected in BALB/c liver tissue. In contrast, in SJL/J mice, low levels of *Bgp2* mRNA expression are found in both the colon and liver. The factors that regulate the differential expression of *Bgp1* and *Bgp2* transcripts in different murine tissues are not yet understood. The expression of Bgp1 proteins on membranes of cells from various tissues and cell lines appears to be required for susceptibility to MHV infection (10–12, 45, 47–49), and high levels of receptor glycoprotein are found on intestine and liver tissues, which are two of the principal target tissues for MHV infection (45). Expression of the Bgp2 protein in murine tissues or cell lines could serve either as an alternative receptor for MHV or as a factor that might modify the expression or functions of Bgp1 proteins.

Role of the Bgp2 protein as a receptor for MHV. The expression of Bgp2 protein in hamster cells transfected with *Bgp2* cDNA made the cells susceptible to infection with MHV-A59, MHV-3, and MHV-JHM. Thus, the Bgp2 protein can serve as a functional receptor for MHV. It is important to note, however, that the Bgp2 protein was not as efficient a receptor for MHV as were the proteins encoded by the $Bgp1^a$

cDNAs when expressed in BHK cells under the control of the same promoter. The percentage of *Bgp2*-transfected cells that synthesized viral proteins following challenge with MHV was much lower than that of *Bgp1*-transfected cells. When Bgp2 is expressed under the control of its natural promoter in murine tissues, there may not be enough of this inefficient receptor to permit infection with MHV virions. An inefficient receptor might play a role in cell-to-cell spread of virus infection after initial infection mediated by Bgp1 proteins. Because virus-infected cells present much more of the viral fusion glycoprotein, S, on their membranes than do virions, infected cells may be able to fuse with cells that express low levels of an inefficient receptor, even though they are resistant to infection by virions. Bgp2 may be expressed in cell types that do not express Bgp1 and could serve as an alternative receptor permitting cell-to-cell spread of virus infection in vivo.

In CMT-93 cells which express both *Bgp1*^{a} and *Bgp2* transcripts, MHV infection can be completely blocked by pretreatment of the cells with anti-Bgp1^a MAb CC1, which does not recognize the N-terminal domain of the Bgp2 protein in immunoblots. Thus, in CMT-93 cells, the only functional receptor is the Bgp1^a protein. Possibly the virus-binding domain of the Bgp2 protein is somehow masked on the surface of CMT-93 cells, perhaps by an excess of a longer Bgp1 protein. Alternatively, the monoclonal antibody might affect the potential receptor function of the Bgp2 protein indirectly, if it is closely associated with Bgp1 proteins that are blocked by the antibody. It is not yet known whether the Bgp1 and Bgp2 protein isoforms are physically associated in the membranes of murine cells or tissues.

CEA-related glycoproteins are expressed on epithelial surfaces of the gastroenteric and respiratory tracts, which are major portals for entry of viruses and other pathogens. An *E. coli* strain was shown to use a human CEA protein as an adhesion factor in the intestine (19), and MHV strains use the murine Bgps as receptors. There is a great variety of CEA-related glycoproteins which are expressed by complex splicing patterns from many closely related genes. In humans, 22 CEA-related genes are clustered on chromosome 19 (40). In the mouse, CEA-related genes include the *Bgp1* and *Bgp2* genes; another *Bgp*-related, but as yet unidentified, gene indicated by the Southern blots shown in Fig. 1; and genes that encode pregnancy-specific glycoproteins (11, 22, 23, 31, 41). Because of the high degree of sequence homology among murine CEA-related glycoproteins, RT-PCR can result in simultaneous amplification of transcripts from several different genes as shown in Fig. 4. In order to avoid confusion in interpreting data concerning the CEA-related glycoproteins expressed in different murine tissues or cell lines, it is necessary to sequence the PCR products and/or to use allele- and gene-specific probes to identify the transcripts. Given the complex, temporally regulated, and tissue-specific patterns of expression of the many structurally similar CEA-related murine glycoproteins, defining the number of isoforms that can serve as MHV receptors and determining their roles in virus infection in vivo constitute an exciting challenge.

ACKNOWLEDGMENTS

Patrick Nédellec and Gabriela Dveksler contributed equally to the work, and both should be considered first authors.

We are greatly indebted to Ed Geissler for providing the mouse cosmid library; to Daniele Malo, Philippe Gros, and Wolfgang Zimmermann for many helpful discussions on gene characterization; and to Marion J. Fultz, Christine B. Cardellichio, and Charles A. Scanga for technical assistance.

Patrick Nédellec is a recipient of studentships from Institut Mérieux, Lyon, France, and from the McGill University Faculty of Medicine. Nicole Beauchemin is a scholar from the Fonds de la Recherche en Santé du Québec. This work was supported by Medical Research Council of Canada grants PG-11410 and MT-12236, by National Institutes of Health grants AI-26075 and AI-25231, and by Uniformed Services University of the Health Sciences grant CO74ET.

REFERENCES

1. **Afar, D. E. H., C. P. Stanners, and J. C. Bell.** 1992. Tyrosine phosphorylation of biliary glycoprotein, a cell adhesion molecule related to carcinoembryonic antigen. Biochim. Biophys. Acta **1134**:46–52.
2. **Barnett, T., A. Kretschmer, D. A. Austen, S. J. Goebel, J. T. Hart, J. J. Elting, and M. E. Kamarck.** 1989. Carcinoembryonic antigens: alternative splicing accounts for multiple mRNAs that code for novel members of the carcinoembryonic antigen family. J. Cell Biol. **108**:267–276.
3. **Barnett, T. R., L. Drake, and W. Pickle II.** 1993. Human biliary glycoprotein gene: characterization of a family of novel alternatively spliced RNAs and their expressed proteins. Mol. Cell. Biol. **13**:1273–1282.
4. **Barthold, S. W.** 1986. Mouse hepatitis virus biology and epizootiology, p. 571–601. *In* P. N. Bhatt, R. O. Jacoby, H. C. Morse III, and A. E. New (ed.), Viral and mycoplasmal infections of laboratory rodents. Effects on biomedical research. Academic Press, Inc., Orlando, Fla.
5. **Beauchemin, N., S. Benchimol, D. Cournoyer, A. Fuks, and C. P. Stanners.** 1987. Isolation and characterization of full-length functional cDNA clones for human carcinoembryonic antigen. Mol. Cell. Biol. **7**:3221–3230.
6. **Beauchemin, N., C. Turbide, J. Q. Huang, S. Benchimol, S. Jothy, K. Shirota, A. Fuks, and C. P. Stanners.** 1989. Studies on the function of carcinoembryonic antigen, p. 49–64. *In* A. Yachi and J. E. Shively (ed.), The carcinoembryonic antigen gene family. Elsevier, Amsterdam.
7. **Boyle, J. F., G. G. Weismiller, and K. V. Holmes.** 1987. Genetic resistance to mouse hepatitis virus correlates with absence of virus-binding activity on target tissues. J. Virol. **61**:185–189.
8. **Brattain, M. G., J. Strobel-Stevens, D. Fine, M. Webb, and A. M. Sarrif.** 1980. Establishment of mouse colonic carcinoma cell lines with different metastatic properties. Cancer Res. **40**:2142–2146.
9. **Devereux, J., P. Haeberli, and O. Smithies.** 1984. A comprehensive set of sequence analysis programs for the VAX. Nucleic Acids Res. **12**:387–395.
10. **Dveksler, G. S., C. W. Dieffenbach, C. B. Cardellichio, K. McCuaig, M. N. Pensiero, G.-S. Jiang, N. Beauchemin, and K. V. Holmes.** 1993. Several members of the mouse carcinoembryonic antigen-related glycoprotein family are functional receptors for the coronavirus mouse hepatitis virus-A59. J. Virol. **67**:1–8.
11. **Dveksler, G. S., M. N. Pensiero, C. B. Cardellichio, R. K. Williams, G.-S. Jiang, K. V. Holmes, and C. W. Dieffenbach.** 1991. Cloning of the mouse hepatitis virus (MHV) receptor: expression in human and hamster cell lines confers susceptibility to MHV. J. Virol. **65**:6881–6891.
12. **Dveksler, G. S., M. N. Pensiero, C. W. Dieffenbach, C. B. Cardellichio, A. A. Basile, P. E. Elias, and K. V. Holmes.** 1993. Mouse coronavirus MHV-A59 and blocking anti-receptor monoclonal antibody bind to the N-terminal domain of cellular receptor MHVR. Proc. Natl. Acad. Sci. USA **90**:1716–1720.
13. **Feinberg, A. P., and B. Vogelstein.** 1983. A technique for radiolabeling DNA restriction fragment endonuclease fragments to high specific activity. Anal. Biochem. **132**:6–13.
14. **Feracci, H., T. P. Connoly, R. N. Margolis, and A. L. Hubbard.** 1987. The establishment of hepatocyte cell surface polarity during fetal liver development. Dev. Biol. **123**:73–84.
15. **Hauck, W., P. Nédellec, C. Turbide, C. P. Stanners, T. R. Barnett, and N. Beauchemin.** Transcriptional control of the human biliary glycoprotein gene, a CEA gene family member down-regulated in colorectal carcinomas. Submitted for publication.
16. **Hauck, W., and C. P. Stanners.** Identification of multiple transcription factors regulating the tissue-specific and differentiation-dependent expression of the carcinoembryonic gene. Submitted for publication.

17. **Huang, J. Q., C. Turbide, E. Daniels, S. Jothy, and N. Beauchemin.** 1990. Spatiotemporal expression of murine carcinoembryonic antigen (CEA) gene family members during mouse embryogenesis. Development **110:**573–588.
18. **Kuroki, M., F. Arakawa, Y. Matsuo, S. Oikawa, H. Nakazato, and Y. Matsuoka.** 1991. Three novel molecular forms of biliary glycoprotein deduced from cDNA clones from a human leukocyte library. Biochem. Biophys. Res. Commun. **176:**578–585.
19. **Leusch, H. G., Z. Drzenick, Z. Markos-Pusztai, and C. Wagener.** 1991. Binding of *Escherichia coli* and *Salmonella* strains to members of the carcinoembryonic antigen family: differential binding inhibition by aromatic α-glycosides of mannose. Infect. Immun. **59:**2051–2057.
20. **Lin, S. H., and G. Guidotti.** 1989. Cloning and expression of a cDNA coding for rat liver plasma membrane ecto-ATPase: the primary structure of the ecto-ATPase is similar to that of the human biliary glycoprotein 1. J. Biol. Chem. **264:**14408–14414.
21. **Margolis, R. N., S. I. Taylor, D. Seminara, and A. L. Hubbard.** 1985. Identification of pp120, an endogenous substrate for the hepatocyte insulin receptor tyrosine kinase, as an integral membrane glycoprotein of the bile canalicular domain. J. Biol. Chem. **85:**7256–7259.
22. **McCuaig, K., M. Rosenberg, P. Nédellec, C. Turbide, and N. Beauchemin.** 1993. Expression of the *Bgp* gene and characterization of mouse colon biliary glycoprotein isoforms. Gene **127:**173–183.
23. **McCuaig, K., C. Turbide, and N. Beauchemin.** 1992. mmCGM1a: a mouse carcinoembryonic antigen gene family member, generated by alternative splicing, functions as an adhesion molecule. Cell Growth Differ. **3:**165–174.
24. **Najjar, S. M., D. Accili, P. Neubert, J. Jernberg, R. N. Margolis, and S. I. Taylor.** 1993. pp120/EctoATPase, an endogenous substrate of the insulin receptor tyrosine kinase, is expressed as two variably spliced isoforms. J. Biol. Chem. **268:**1201–1206.
24a. **Nédellec, P., et al.** Unpublished data.
25. **Obrink, B.** 1991. C-CAM (Cell-Cam 105)—a member of the growing immunoglobulin superfamily of cell adhesion proteins. Bioessays **13:**227–234.
26. **Ocklind, C., and B. Obrink.** 1982. Intercellular adhesion of rat hepatocytes: identification of a cell surface glycoprotein involved in the initial adhesion process. J. Biol. Chem. **257:**6788–6795.
27. **Oikawa, S., C. Inusuka, M. Kuroki, F. Arakawa, Y. Matsuoka, G. Kosaki, and H. Nakazato.** 1991. A specific heterotypic cell adhesion activity between members of carcinoembryonic antigen family, W272 and NCA, is mediated by N-domains. J. Biol. Chem. **266:**7995–8001.
28. **Robbins, J., P. F. Robbins, C. A. Kozak, and R. Callahan.** 1991. The mouse biliary glycoprotein gene (*Bgp*): partial nucleotide sequence, expression, and chromosomal assignment. Genomics **10:**583–587.
29. **Rojas, M., A. Fuks, and C. P. Stanners.** 1990. Biliary glycoprotein, a member of the immunoglobulin supergene family, functions *in vitro* as a Ca^{2+}-dependent intercellular adhesion molecule. Cell Growth Differ. **1:**527–533.
30. **Rosenberg, M., P. Nédellec, S. Jothy, D. Fleiszer, C. Turbide, and N. Beauchemin.** 1993. Expression of mouse biliary glycoprotein, a carcinoembryonic antigen-related gene, is downregulated in malignant mouse tissues. Cancer Res. **53:**4938–4945.
31. **Rudert, F., A. M. Saunders, S. Rebstock, J. A. Thompson, and W. Zimmermann.** 1992. Characterization of murine carcinoembryonic antigen gene family members. Mamm. Genome **3:**262–273.
32. **Sambrook, J., E. F. Fritsch, and T. Maniatis.** 1989. Molecular cloning: a laboratory manual, 2nd ed. Cold Spring Harbor Laboratory Press, Cold Spring Harbor, N.Y.
33. **Sanger, F., S. Nicklen, and A. R. Coulson.** 1977. DNA sequencing with chain-terminating inhibitors. Proc. Natl. Acad. Sci. USA **74:**5463–5467.
34. **Schrewe, H., J. Thompson, M. Bona, L. J. F. Hefta, A. Maruya, M. Hassauer, J. E. Shively, S. von Kleist, and W. Zimmermann.** 1990. Cloning of the complete gene for carcinoembryonic antigen: analysis of its promoter indicates a region conveying cell type-specific expression. Mol. Cell. Biol. **10:**2738–2748.
35. **Sippel, C. J., F. J. Suchy, M. Ananthanarayanan, and D. H. Perlmutter.** 1993. The rat liver ecto-ATPase is also a canalicular bile acid transport protein. J. Biol. Chem. **268:**2083–2091.
36. **Smith, A. L., C. B. Cardellichio, D. F. Vinograd, M. S. deSouza, S. W. Barthold, and K. V. Holmes.** 1991. Monoclonal antibody to the receptor for murine coronavirus MHV-A59 inhibits virus replication in vivo. J. Infect. Dis. **163:**879–882.
37. **Spaan, W. J. M., P. J. M. Rottier, M. C. Horzinek, and B. A. M. Van Der Zeijst.** 1981. Isolation and identification of virus-specific mRNAs in cells infected with mouse hepatitis virus (MHV-A59). Virology **108:**424–434.
38. **Sturman, L. S., and K. K. Takemoto.** 1972. Enhanced growth of a murine coronavirus in transformed mouse cells. Infect. Immun. **6:**501–507.
39. **Svalander, P. C., P. Odin, B. O. Nilsson, and B. Obrink.** 1990. Expression of CellCAM-105 in the apical surface of rat uterine epithelium is controlled by ovarian steroid hormones. J. Reprod. Fert. **88:**213–221.
40. **Thompson, J. A., F. Grunert, and W. Zimmermann.** 1991. Carcinoembryonic antigen gene family: molecular biology and clinical perspectives. J. Clin. Lab. Invest. **5:**344–366.
41. **Turbide, C., M. Rojas, C. P. Stanners, and N. Beauchemin.** 1991. A mouse carcinoembryonic antigen gene family member is a calcium-dependent cell adhesion molecule. J. Biol. Chem. **266:**309–315.
42. **Wege, H., S. Siddell, and V. ter Meulen.** 1982. The biology and pathogenesis of coronaviruses. Curr. Top. Microbiol. Immunol. **99:**165–200.
43. **Willcocks, T. C., and I. W. Craig.** 1990. Characterization of the genomic organization of human carcinoembryonic antigen (CEA): comparison with other family members and sequence analysis of 5′ controlling region. Genomics **8:**492–500.
44. **Williams, A. F., and A. N. Barclay.** 1988. The immunoglobulin superfamily: domains for cell surface recognition. Annu. Rev. Immunol. **6:**381–405.
45. **Williams, R. K., G.-S. Jiang, and K. V. Holmes.** 1991. Receptor for mouse hepatitis virus is a member of the carcinoembryonic antigen family of glycoproteins. Proc. Natl. Acad. Sci. USA **88:**5533–5536.
46. **Williams, R. K., G.-S. Jiang, S. W. Snyder, M. F. Frana, and K. V. Holmes.** 1990. Purification of the 110-kilodalton glycoprotein receptor for mouse hepatitis virus (MHV)-A59 from mouse liver and identification of a nonfunctional, homologous protein in MHV-resistant SJL/J mice. J. Virol. **64:**3817–3823.
47. **Yokomori, K., M. Asanaka, S. A. Stohlman, and M. M. C. Lai.** 1993. A spike protein-dependent cellular factor other than the viral receptor is required for mouse hepatitis virus entry. Virology **196:**45–56.
48. **Yokomori, K., and M. M. C. Lai.** 1992. Mouse hepatitis virus utilizes two carcinoembryonic antigens as alternative receptors. J. Virol. **66:**6194–6199.
49. **Yokomori, K., and M. M. C. Lai.** 1992. The receptor for mouse hepatitis virus in the resistant mouse strain SJL is functional: implications for the requirement of a second factor for viral infection. J. Virol. **66:**6931–6938.
50. **Zhou, H., A. Fuks, G. Alcaraz, T. J. Bolling, and C. P. Stanners.** 1993. Homophilic adhesion between Ig superfamily carcinoembryonic antigen molecules involves double reciprocal bonds. J. Cell Biol. **122:**951–960.